Toxicology in Vitro 55 (2019) 62–74

Contents lists available at ScienceDirect

Toxicology in Vitro

journal homepage: www.elsevier.com/locate/toxinvit

Habu coagulotoxicity: Clinical implications of the functional diversification of *Protobothrops* snake venoms upon blood clotting factors

Jordan Debono[a], Mettine H.A. Bos[b], Amanda Nouwens[c], Lilin Ge[d,e], Nathaniel Frank[f], Hang Fai Kwok[d,*], Bryan G. Fry[a,*]

[a] Venom Evolution Lab, School of Biological Sciences, University of Queensland, St Lucia, QLD 4072, Australia
[b] Division of Thrombosis and Hemostasis, Einthoven Laboratory for Vascular and Regenerative Medicine, Leiden University Medical Center, Albinusdreef 2, 2333 ZA, Leiden, the Netherlands
[c] School of Chemistry and Molecular Biosciences, University of Queensland, St. Lucia 4072, Australia
[d] Institute of Translational Medicine, Faculty of Health Sciences, University of Macau, Avenida da Universidade, Taipa, Macau, China
[e] Jiangsu Key Laboratory for Functional Substance of Chinese Medicine, School of Pharmacy, Nanjing University of Chinese Medicine, 138 Xianlin Avenue, Qixia District, Nanjing 215400, China
[f] Mtoxins, 1111 Washington Ave, Oshkosh, WI 54901, USA

A B S T R A C T

Venom can affect any part of the body reachable via the bloodstream. Toxins which specifically act upon the coagulation cascade do so either by anticoagulant or procoagulant mechanisms. Here we investigated the coagulotoxic effects of six species within the medically important pit viper genus *Protobothrops* (Habu) from the Chinese mainland and Japanese islands, a genus known to produce hemorrhagic shock in envenomed patients. Differential coagulotoxicity was revealed: *P. jerdonii* and *P. mangshanensis* produced an overall net anticoagulant effect through the pseudo-procoagulant clotting of fibrinogen; *P. flavoviridis* and *P. tokarensis* exhibit a strong anticoagulant activity through the destructive cleavage of fibrinogen; and while *P. elegans* and *P. mucrosquamatus* both cleaved the A-alpha and B-beta chains of fibrinogen they did not exhibit strong anticoagulant activity. These variations in coagulant properties were congruent with phylogeny, with the closest relatives exhibiting similar venom effects in their action upon fibrinogen. Ancestral state reconstruction indicated that anticoagulation mediated by pseudo-procoagulant cleavage of fibrinogen is the basal state, while anticoagulation produced by destructive cleavage of fibrinogen is the derived state within this genus. This is the first in depth study of its kind highlighting extreme enzymatic variability, functional diversification and clotting diversification within one genus surrounding one target site, governed by variability in co-factor dependency. The documentation that the same net overall function, anticoagulation, is mediated by differential underlying mechanics suggests limited antivenom cross-reactivity, although this must be tested in future work. These results add to the body of knowledge necessary to inform clinical management of the envenomed patient.

1. Introduction

Venom is defined as a secretion produced in specialised cells that is delivered to a target animal through a wound, and consequently disrupts normal physiological or biochemical processes (Fry et al., 2009a; Fry et al., 2009b; Jackson and Fry, 2016; Jackson et al., 2017; Nelsen et al., 2014). Venoms are complex mixtures of enzymes, toxins, peptides, organic molecules and salts (Fry et al., 2009a; Fry et al., 2009b) which are used to facilitate feeding, (Fry et al., 2008; Fry et al., 2013; Fry et al., 2009b; Jackson et al., 2013) defence such as that found in spitting cobras (Cascardi et al., 1999; Hayes et al., 2008; Panagides et al., 2017) or competition (Deufel and Cundall, 2003) for the producing organism (Fry and Wüster, 2004; Sunagar et al., 2013). Numerous studies have demonstrated that venom genes evolve at a much faster rate than housekeeping genes, facilitating a drive towards a highly specialised and complex venom composition (Casewell et al., 2013; Jackson et al., 2013; Sunagar et al., 2013; Vonk et al., 2013). This facilitated diversification allows toxins within venom to evolve rapidly, and at different rates, through a variety of different selective mechanisms. These mechanisms include, but are not limited to, ecological niche occupation, which is in-turn directly related to prey ecology, and in some cases taxon-specific toxins including the potential for prey escape or prey retaliation (Daltry et al., 1996; Fry et al., 2013; Jackson et al., 2013; Koludarov et al., 2014; Li et al., 2005; Pawlak et al., 2006; Pawlak et al., 2009; Sunagar et al., 2013; Sunagar et al., 2014; Yang et al., 2016).

Snake venoms are made up of a myriad of mutated protein families, each responsible for varying pathophysiological effects (Fry, 2005). Coagulatoxins target the blood coagulation cascade via one of two mutually exclusive functional mechanisms: anticoagulation or procoagulation (Fry et al., 2009a). Anticoagulation that is mediated via proteolytic cleavage is accomplished through two different mechanisms:

* Corresponding authors.
E-mail addresses: hfkwok@umac.mo (H.F. Kwok), bgfry@uq.edu.au (B.G. Fry).

https://doi.org/10.1016/j.tiv.2018.11.008
Received 29 August 2018; Received in revised form 24 October 2018; Accepted 20 November 2018
Available online 22 November 2018
0887-2333/

cleavage in a non-clotting, destructive manner which results in direct anticoagulation; or cleavage in a pseudo-procoagulant manner, resulting in weak fibrin clots with very short-half lives. While kallikrein-type serine proteases and snake venom metalloproteases (SVMP) both may cleave fibrinogen in a non-clotting, destructive manner (Casewell et al., 2015; Vaiyapuri et al., 2015), only kallikrein toxins are currently known for the pseudo-procoagulant activity.

Fibrinogen is a trinodular protein, present in high concentrations in plasma (Wolberg, 2007), and is made up of three polypeptide chains (Aα, Bβ, γ). Under normal cleavage by thrombin, fibrinopeptides A and B are cleaved from the Aα and Bβ chains, thereby exposing the γ chain and producing strong, well-ordered lattices. These fibrin clots are further strengthened by thrombin-mediated activation of Factor XIII into FXIIIa, with FXIIIa in turn additionally cross linking the fiber strands (Bagoly et al., 2012; Collet et al., 2000; Koh and Kini, 2012; Longstaff and Kolev, 2015; Ryan et al., 1999; Wolberg, 2007). When fibrinogen is cleaved by snake venom in a non-clotting manner, SVMPs cleave the Aα-chain while kallikreins cleave the Bβ-chain (Kini, 2005; Kini and Koh, 2016; Sajevic et al., 2011; Swenson and Markland, 2005) with both cleaving at sites distinct from that of thrombin. In contrast, when fibrinogen is cleaved in a pseudo-procoagulant manner by venom kallikreins, fibrinopeptides A or B (or both) are cleaved from their respective chains but through aberrant cleavage sites, resulting in disordered lattice-works and weak, short-lived clots (Sajevic et al., 2011; Swenson and Markland, 2005).

The wide-ranging Asian pit viper genus *Protobothrops* occupies the islands of Japan, mainland China and islands off China, with the occupation of diverse ecological niches mirrored by diverse morphology. *Protobothrops* bites are known for potent haemorrhagic shock effects in prey and human bite victims (Chen et al., 2009; Nishimura et al., 2016). Target sites include impeding primary haemostasis by disruption along the cascade from the blockage of platelet aggregation through to inhibiting clot formation due to the unnatural cleavage of fibrinogen (Collet et al., 2000; Kolev and Longstaff, 2016; Longstaff and Kolev, 2015; Mosesson, 2005).

Despite the medical importance of these snakes, a comprehensive examination of intra-genus venom variation has not been undertaken. Such data will provide fundamental information which may aid the prediction of clinical effects and thus guide snake bite case management. This study used a myriad of techniques to investigate the effects of six *Protobothrops* venoms upon the clotting cascade, with a particular focus upon their actions upon fibrinogen.

2. Materials and methods

A multidisciplinary approach was used to investigate the functional variability of a range of representative species from the Asian pit viper genus *Protobothrops*. Venom samples from six *Protobothrops* species were from captive snakes: *P. elegans* (unknown locality founding stock), *P. flavoviridis* (Okinowa, Japan founding stock), *P. jerdonii* (Chinese founding stock), *P. mangshanensis* (Mt Mang, Hunan, China founding stock), *P. mucrosquamatus* (Sa Pa, Vietnam founding stock) and *P. tokarensis* (Tokara Island, Japan founding stock). Human plasma was obtained from the Australian Red Cross (Research agreement #18-03QLD-09 and University of Queensland Human Ethics Committee Approval #2016000256). All plasma was prepared as 3.2% citrated stock, aliquoted into 1 ml quantities, which were snap frozen in liquid nitrogen, and stored in a − 80 freezer until needed, at which time an aliquot was defrosted by placing into a 37 °C water bath for 10 min. All venom and plasma work was undertaken under the University of Queensland Biosafety Approval #IBC134BSBS2015.

2.1. Enzyme assays

2.1.1. Fluorescent substrate activation

In order to investigate variation in enzymatic activities, artificial substrates were used as previously described by us (Debono et al., 2017). 1 mg/ml stock solutions were made by reconstituting freeze dried venom in 50% deionised water/50% glycerol (> 99.9%, Sigma, St Louis, MO, USA) at a 1:1 ratio to preserve enzymatic activity and reduce enzyme degradation. This stock solution was diluted with enzyme buffer for use in assays.

For metalloprotease and serine protease assays, varying concentrations of crude venom (10 ng/μl and 50 ng/μl) were plated out in triplicates on a 384-well plate (black, Lot#1171125, nunc™ Thermo Scientific, Rochester, NY, USA) and measured by adding 90 μl quenched fluorescent substrate per well (total volume 100 μl/well, 10 μl/5 ml enzyme buffer, 150 mM NaCl, and 50 mM Tri-HCl (pH 7.3), Fluorogenic Peptide Substrate, R & D systems, Cat#ES001, ES003, ES005, ES010, ES011, Minneapolis, Minnesota). Fluorescence was monitored by a Fluoroskan Ascent™ (Thermo Scientific, Vantaa, Finland) Microplate Fluorometer (Cat#1506450, Thermo Scientific, Vantaa, Finland) with the wavelengths of excitation of 320 nm, emission at 405 nm for Cat#ES001, ES003, ES005, ES010, and 390 nm, emission at 460 nm for Cat#ES011, run over 400 mins or until activity had ceased. Data was collected using Ascent® Software v2.6 (Thermo Scientific, Vantaa, Finland).

For phospholipase A_2 (PLA_2) assays we assessed the venoms using a fluorescence substrate assay (EnzChek® Phospholipase A_2 Assay Kit, Cat#E10217, Thermo Scientific, Rochester, NY, USA), measured on a Fluoroskan Ascent® Microplate Fluorometer (Cat#1506450, Thermo Scientific, Vantaa, Finland). Venom was brought up in 12.5 μl 1 × PLA_2 reaction buffer (50 mM Tris-HCL, 100 mM NaCl, 1 mM $CaCl_2$, pH 8.9), thus being diluted to (50 ng/μl), and plated out in triplicates on a 384-well plate (black, Lot#1171125, nunc™ Thermo Scientific, Rochester, NY, USA). The triplicates were measured by dispensing 12.5 μl quenched 1 mM EnzChek® (Thermo Scientific, Rochester, NY, USA) Phospholipase A_2 Substrate per well (total volume 25 μl/well) over 100 min or until activity had ceased (at an excitation of 485 nm, emission 538 nm). Purified PLA_2 from bee venom (1 U/ml) was used as a positive control and data was collected using Ascent® Software v2.6 (Thermo Scientific, Vantaa, Finland).

2.1.2. Plasminogen activation

1 mg/ml venom stock solutions were combined with enzyme buffer to make the following dilutions: 10 ng/μl, 50 ng/μl and 100 ng/μl. These varying concentrations of enzyme activity in venom were plated out on a 384-well plate (black, Lot#1171125, nunc™ Thermo Scientific, Rochester, NY, USA) in triplicates, with and without 10 ng/μl plasminogen per well (Lot#FF0125 HCPG-0130, Haematologic Technologies Inc., Essex Junction, VT, USA). Plasminogen, a serine protease, can be activated by a serine protease specific substrate (Fluorogenic Peptide Substrate, R & D systems, Cat# ES011, Minneapolis, Minnesota). Plasmin was used as a positive control (10 ng/μl per positive control well, Lot#EE1120, HCPM-0140, Haematologic Technologies Inc., Essex Junction, VT, USA). Activation from venoms was measured by adding 90 μl quenched fluorescent substrate per well (total volume 100 μl/well; 20 μl/5 ml enzyme buffer - 150 mM NaCl and 50 mM Tri-HCl (pH 7.3), Fluorogenic Peptide Substrate, R & D systems, Cat#ES011, Minneapolis, Minnesota). Fluorescence was monitored by a Fluoroskan Ascent™ Microplate Fluorometer (Cat#1506450, Thermo Scientific, Vantaa, Finland) at excitation 390 nm and emission at 460 nm over 150mins or until activity had ceased. Data was collected using Ascent® Software v2.6 (Thermo Scientific, Vantaa, Finland). Experiments were conducted in triplicate.

2.1.3. Prothrombin activation

The ability of *Protobothrops* crude venom to directly activate prothrombin was investigated and measured by modifying the above protocol used for plasminogen activation. Plasminogen was replaced with prothrombin (Lot#EE0930, HCP-0010, Haematologic Technologies Inc., Essex Junction, VT, USA) and plasmin was replaced

with thrombin (Lot#FF0315, HCT-0020, Haematologic Technologies Inc., Essex Junction, VT, USA) as a positive control (10 ng/μl per positive control well). Data was collected using Ascent® Software v2.6 (Thermo Scientific, Vantaa, Finland). Experiments were conducted in triplicate.

2.1.4. Factor X activation

The ability for *Protobothrops* crude venom to directly activate blood coagulation Factor X (FX) was investigated and measured by modifying the above protocol used for plasminogen activation using FX (Lot#FF0407, HCX-0050, Haematologic Technologies Inc., Essex Junction, VT, USA) as the experimental target and FXa (Lot#EE1102, HCXA-0060, Haematologic Technologies Inc., Essex Junction, VT, USA) as the positive control (10 ng/μl per positive control well). Data was collected using Ascent® Software v2.6 (Thermo Scientific, Vantaa, Finland). Experiments were conducted in triplicate.

2.1.5. Protein C activation

The ability for *Protobothrops* crude venom to directly activate Protein C was investigated and measured by modifying the above protocol used for plasminogen activation. Plasminogen was replaced with Protein C (Lot#FF0802, HCPC-0070, Haematologic Technologies Inc., Essex Junction, VT, USA) and plasmin was replaced with activated Protein C (Lot#FF0325, HCAPC-0080, Haematologic Technologies Inc., Essex Junction, VT, USA) as a positive control (10 ng/μl per positive control well). Data was collected using Ascent® Software v2.6 (Thermo Scientific, Vantaa, Finland). Experiments were conducted in triplicate.

2.1.6. Phylogenetic comparative analyses

Observed venom activities of the different snake species were investigated in an evolutionary framework by mapping them on a taxonomical tree (phylogeny as per Alencar et al., 2016), generated using the Mesquite software package and analyses subsequently performed using the R package Phytools using Phylogenetic Generalized Least Squares (PGLS) (Lister et al., 2017; Rogalski et al., 2017). Analyses were implemented in R v3.2.5 (Team, 2016) using the APE package for basic data manipulation (Paradis et al., 2004). Ancestral states of each substrate functional trait (ES001, ES002, ES003, ES005, ES010, ES011, PLA_2, coagulation) were estimated via maximum likelihood with the contMap function in phytools (Revell, 2012).

2.2. Coagulation analysis

2.2.1. Action upon plasma

2.2.1.1. Plasma clotting and co-factor dependency of Ca^{2+} and phospholipid. As per (Debono et al., 2017), in order to investigate whole plasma clotting and co-factor dependency clotting, we prepared healthy human plasma (citrate 3.2%, Lot#1690252, approval # 16-04QLD-10), obtained from the Australian Red Cross (44 Musk Street, Kelvin Grove, Queensland 4059). Coagulotoxic effects were measured by a modified procoagulant protocol on a Stago STA-R Max coagulation robot (France) using Stago Analyser software v0.00.04 (Stago, Asniéres sur Seine, France). Plasma clotting baseline parameters were determined by performing the standardised activated Partial Thromboplastin Time (aPTT) test (Stago Cat# T1203 TriniCLOT APTT HS). This was used as a control to determine the health of the plasma according to the universal standard range of between 27 and 35 s. Plasma aliquots of 2 ml, which had been flash frozen in liquid nitrogen and stored in a − 80 °C freezer, were defrosted in an Arctic refrigerated circulator SC150-A40 at 37 °C. In order to determine the ability of the venom to clot the plasma, a starting volume of 50 μl of crude venom (100 μg/ml concentration) was diluted with STA Owren Koller Buffer (Stago Cat# 00360) to produce an 8-dilution series of 20, 10, 4, 1.6, 0.66, 0.25, 0.125, and 0.05 μg/ml final reaction concentrations, which were performed in triplicate. $CaCl_2$ (50 μl; 25 mM stock solution Stago Cat# 00367 STA $CaCl_2$ 0.025 M) was added along with 50 μl phospholipid (solubilized in Owren Koller Buffer adapted from STA C·K Prest standard kit, Stago Cat# 00597). An additional 25 μl of Owren Koller Buffer was added to the cuvette and incubated for 120 s at 37 °C before adding 75 μl of human plasma. Relative clotting was then monitored for 999 s or until plasma clotted (whichever was sooner). Additional tests were run, both with and without $CaCl_2$ and phospholipid, respectively, to test for $CaCl_2$ or phospholipid dependency, with STA Owren Koller Buffer was used as a substitute, using the same volumes to allow for consistency in the final volumes (250 μl).

2.2.1.2. Plasma anticoagulant inhibition – FXa and thrombin. The ability for *Protobothrops* crude venom to directly prevent a fibrin clot from forming by inhibiting FXa or thrombin was investigated. Species were those which were unable to clot plasma in the above assay (1A). Clotting baseline parameters were established by performing FXa-initiated clotting in human plasma utilising liquid FXa from Stago Liquid Anti FXa kit (Stago Cat#250491 Liquid Anti FXa kit). This was used as a control to determine the normal clotting of plasma caused by the activation of prothrombin via FXa under these specific conditions (result: 12.5 ± 0.2 s). A starting volume of 50 μl of crude venom (at 10 mg/ml) was diluted with STA Owren Koller Buffer (Stago Cat# 00360). An 8-dilution series of 20, 10, 4, 1.6, 0.66, 0.25, 0.125, and 0.05 μg/ml final reaction concentrations was performed in triplicate. Following, 50 μl $CaCl_2$ (25 mM stock solution Stago Cat# 00367 STA) was added to 50 μl phospholipid (solubilized in Owren Koller Buffer adapted from STA C·K Prest standard kit, Stago Cat# 00597) and 50 μl Factor Xa (unknown concentration from supplier, Liquid Anti-Xa FXa Cat#253047, Stago) or 50 μl TCT thrombin kit (unknown concentration from supplier, Thrombin, Lot#252818, Stago) and incubated for 120 s. Post incubation 50 μl of either human plasma for the FXa inhibition test (citrate 3.2%, Lot#1690252, approval # 16-04QLD-10, obtained from the Australian Red Cross (44 Musk Street, Kelvin Grove, Queensland 4059) (defrosted in an Arctic refrigerated circulator SC150-A40 at 37 °C)) or human fibrinogen for the thrombin inhibition test (at 4 mg/ml, (Lot#F3879, Sigma Aldrich, St. Louis, Missouri, United States, reconstituted in enzyme buffer (150 mM NaCl and 50 mM Tri-HCl (pH 7.3)) was added to the reaction and each test run in triplicate for each concentration. Relative clotting was then monitored for 999 s or until plasma clotted (whichever was sooner) on a Stago STA-R Max coagulation robot (France) using Stago Analyser software v0.00.04 (Stago, Asniéres sur Seine, France). Additional tests were run with increased incubation times of 300 s and 600 s. Venom dilutions in triplicates were mapped over time using GraphPad PRISM 7.0 (GraphPad Prism Inc., La Jolla, CA, USA) to produce concentration curves.

2.2.2. Action upon fibrinogen

2.2.2.1. Fibrinogen clotting and co-factor dependency of Ca^{2+} and phospholipid. The ability for *Protobothrops* crude venom to directly clot human fibrinogen was investigated and measured by following that described by Debono et al., 2017, with human fibrinogen (4 mg/ml, Lot#F3879, Sigma Aldrich, St. Louis, Missouri, United States) used in place of human plasma. Relative clotting was then monitored for 999 s or until fibrinogen clotted (whichever was sooner). Experiments were conducted in triplicate. Venom dilutions in triplicates were mapped over time using GraphPad PRISM 7.0 (GraphPad Prism Inc., La Jolla, CA, USA) to produce concentration curves.

2.2.2.2. Thromboelastography® 5000. The strength of clots formed by *Protobothrops* venom on human fibrinogen (4 mg/ml) and human plasma for pseudo-procoagulant venoms, or the decrease in thrombin-incuded clot strength for anticoagulant venoms, was investigated using a Thrombelastogram® 5000 Haemostasis analyser (Haemonetics®, Haemonetics Australia Pty Ltd., North Rdye, Sydney 2113, Australia). Human fibrinogen (4 mg/ml, Lot#F3879, Sigma Aldrich, St. Louis,

Missouri, United States) was reconstituted in enzyme buffer (150 mM NaCl and 50 mM Tri-HCl (pH 7.3)). Natural pins and cups (Lot# HMO3163, Haemonetics Australia Pty Ltd., North Rdye, Sydney 2113, Australia) were used. The same stoichiometry as for the clotting time tests (4.1) was maintained, with the volumes proportionally changed to accommodate the larger reaction volume: 7 µl of the 1 mg/ml venom working stock or 7 µl thrombin as a positive control (stable thrombin from Stago Liquid Fib kit, unknown concentration from supplier (Stago Cat#115081 Liquid Fib)), 72 µl $CaCl_2$ (25 mM stock solution Stago Cat# 00367 STA), 72 µl phospholipid (solubilized in Owren Koller Buffer adapted from STA C·K Prest standard kit, Stago Cat# 00597), and 20 µl Owren Koller Buffer (Stago Cat# 00360) was combined with 189 µl fibrinogen or human plasma and run immediately for 30 mins to allow for ample time for clotting formation. An additional positive control of 7 µl Factor Xa (unknown concentration from supplier, Liquid Anti-Xa FXa Cat#253047, Stago) was also incorporated for plasma only. For assays in which no clot was formed, tests for anticoagulant non-clotting cleavage of fibrinogen were undertaken by the addition of 7 µl thrombin to generate a clot and to determine the effects of fibrinogen degradation.

2.2.2.3. Fibrinogen gels. To investigate fibrinogenolysis activity demonstrating α, β and γ chain cleavage, 1D SDS PAGE 12% acrylamide gels were cast, run and stained following the protocol described in (Ali et al., 2013; Debono et al., 2017) outlining 1D SDS PAGE preparation and running conditions.

Human fibrinogen (Lot#F3879, Sigma Aldrich, St. Louis, Missouri, United States) was reconstituted to a concentration of 1 mg/ml in isotonic saline solution, flash frozen in liquid nitrogen and stored at −80 °C until use. Freeze-dried venom was reconstituted in deionised H_2O and concentrations were measured using a Thermo Fisher Scientific™ NanoDrop 2000 (Waltham, MA, USA). Assay concentrations were a 1:10 ratio of venom:fibrinogen. Human fibrinogen (Lot#F3879, Sigma Aldrich, St. Louis, Missouri, United States) stock of 1 mg/ml was dispensed into ten 120 µl aliquots. Fibrinogen from each aliquot (10 µl) was added to 10 µl buffer dye (5 µl of 4× Laemmli sample buffer (Bio-Rad, Hercules, CA, USA), 5 µl deionised H_2O, 100 mM DTT (Sigma-Aldrich, St. Louis, MO, USA)) as an untreated control lane. An additional fibrinogen aliquot (10 µl) was firstly incubated for 60 mins at 37 °C before immediately adding 10 µl buffer dye. Venom stock (1 µl at 1 mg/ml) was added to the remaining 100 µl fibrinogen aliquot and incubated over 60 mins at 37 °C, taking out 10 µl at varying time points (1, 5, 10, 15, 20, 30, 45, and 60 mins). This 10 µl was immediately added to an additional 10 µl buffer dye. Once all 8-time points including the two controls were added to the buffer dye these were incubated at 100 °C for 4 min then immediately loaded into the precast 1D SDS-PAGE gel. The following set up within the gel was as follows: Lane 1: untreated, unincubated fibrinogen, Lane 2: 1-min 37 °C incubation, Lane 3: 5 min 37 °C incubation, Lane 4: 10 min 37 °C incubation, Lane 5: 15 min 37 °C incubation, Lane 6: 20 min 37 °C incubation, Lane 7: 30 min 37 °C incubation, Lane 8: 45 min 37 °C incubation, Lane 9: 60 min 37 °C incubation, Lane 10: untreated fibrinogen that has been incubated for 60 min at 37 °C. Gels were prepared in triplicate under the described conditions per venom and were run in 1× gel running buffer (as described by (Debono et al., 2017; Koludarov et al., 2017) at room temperature at 120 V (Mini Protean3 power-pack from Bio-Rad, Hercules, CA, USA) until the dye front neared the bottom of the gel. Gels were stained with colloidal coomassie brilliant blue G250 (34% methanol (VWR Chemicals, Tingalpa, QLD, Australia), 3% orthophosphoric acid (Merck, Darmstadt, Germany), 170 g/L ammonium sulfate (Bio-Rad, Hercules, CA, USA), 1 g/L Coomassie blue G250 (Bio-Rad, Hercules, CA, USA), and destained in deionised H_2O.

Fibrinogen gel analysis was undertaken using the publicly available software ImageJ (V1.51r, Java 1.6.0_24, National Institutes of Health, Bethesda, Maryland, USA) (Schneider et al., 2012), gels that had been scanned using a standard printer/scanner were loaded onto the software. Gel images were opened in ImageJ and changed to 32 bit to emphasise darken bands of fibrinogen chains. The 'box function' was then used to draw around the control bands selecting all three chains. This was repeated for all 10 treatment lanes. Lanes were then 'plotted' using the 'plot lanes' function which creates a gel band intensity graph. Using the 'line function', lines were drawn between troughs of each band separating the individual peaks and troughs representing the alpha, beta and gamma chains. The intensity represents the amount of protein within that particular band and as the chain degrades the intensity decreases. Using the 'wand function' each peak within the graph was selected automatically producing a quantity for the area under the curve. These values were entered into Windows Excel 2016, average taken and graphed using GraphPad PRISM 7.0 (GraphPad Prism Inc., La Jolla, CA, USA). This process was repeated for all three triplicates for each venom.

2.2.2.4. Fibrinolysis +/− tPA. To investigate the fibrinolysis ability of *Protobothrops* venoms, varying concentrations of venom (100 ng/µl, 500 ng/µl and 1 µg/µl) were tested under varying conditions with the addition of tissue plasminogen activator (tPA, Sekisui Diagnostics, Lexington, MA, USA). Aliquots (100 µl) of normal pooled human plasma (Leiden University Medical Center (Leiden, NL)) stored at −80 °C were defrosted in a water bath at 37 °C. A 96-well plate was prepared under the following conditions: 6 pM tissue factor (TF) (Innovin, Siemens, USA) was added to 10 µM phospholipid vesicles (PCPS, 75% phosphatidylcholine and 25% phosphatidylserine, Avanti Polar Lipids, Alabama, USA) in HEPES buffer (25 mM HEPES, 137 mM NaCl, 3.5 mM KCl, 0.1% BSA (Bovine Serum Albumin A7030, Sigma Aldrich, St Louis, MD, USA)) and gently incubated at 37 °C for 1 h in a water bath. 17 mM CaCl and 37.5 U/ml tPA (diluted in dilution buffer (20 mM HEPES, 150 mM NaCl, 0.1% PEG-8000 (Polyethylene glycol 8000,1,546,605 USP, Sigma Aldrich, St Louis, MD, USA), pH 7.5)) was then added to the solution. A volume of 30 µl of this solution was added to each experimental well, along with 10 µl of venom at varying concentrations and an additional 10 µl of HEPES buffer, prepared on ice (total well volume of 100 µl). Normal pooled plasma (50 µl) was immediately added to each well (heated to 37 °C). Absorbance measuring commenced immediately and was measured every 30 s over 3 h at 405 nm on a Spectra Max M2^e (Molecular Devices, Sunnyvale, CA, USA) plate reader, heated to 37 °C. Measurements were captured on Softmax Pro software (V 5.2, Molecular Devices, Sunnyvale, CA, USA) and data points analysed using GraphPad PRISM 7.0 (GraphPad Prism Inc., La Jolla, CA, USA). All experimental conditions were repeated in triplicates and averaged.

2.2.3. Platelet agglutination and inhibition

The ability to aggregate platelets via the GP Ib/IX receptor was tested for both venoms at varying concentrations (1, 2, and 5 µg/µl) using the ristocetin cofactor assay (Lot# H081032, Chrono-log™, Havertown, PA, USA) under modified conditions. For a control sample, in a modified glass cuvette with a rubber spacer and electrode stir bar, 200 µl of platelets (Lot# 1087–40) reconstituted in TRIS-buffer saline (Lot# 1091–35) was combined with 25 µl Ristocetin (10 mg/ml, Lot# 1088–33), reconstituted in Ultra-pure water. Prior to aggregation tracking performed on a Chrono-log 700 multichannel system (Chrono-log, DKSH, Vic, Australia), 0% and 100% baselines were established. Agglutination of platelets was measured for 6mins under the following conditions: slope length 16, gain 0.05, mode optical. For experimental samples, 200 µl of reconstituted platelets was combined with an additional 40 µl TRIS-buffer saline and incubated at 37 °C for 2mins. After incubation, 10 µl of crude venom/TRIS-buff saline solution at varying concentrations (100 ng/µl, 200 ng/µl and 5 µg/µl) were injected into the cuvette and run for 6 mins under the same conditions. Controls and experimental samples were run in triplicate.

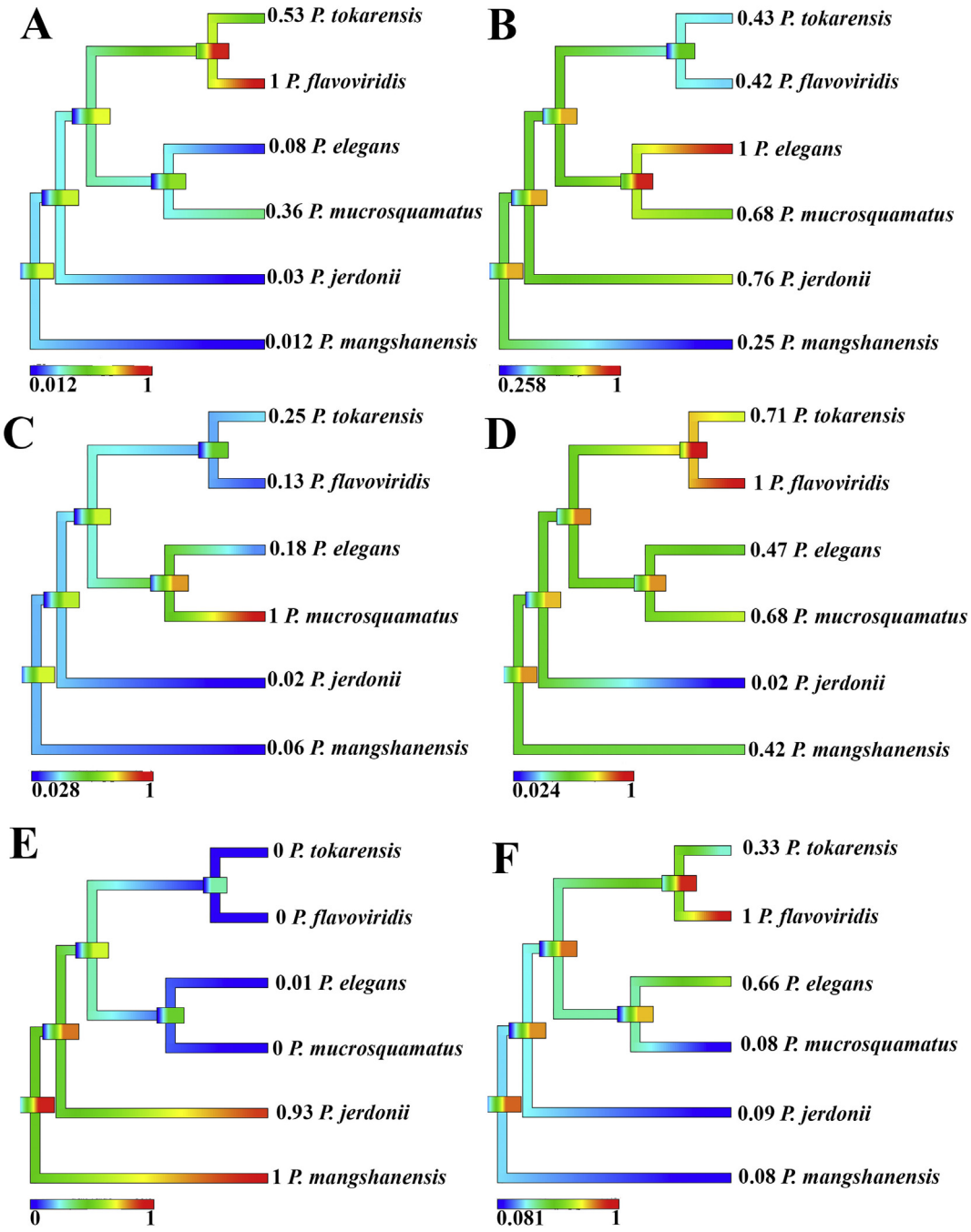

Fig. 1. Ancestral state reconstruction of enzymatic substrate activity of *Protobothrops* species based on their normalised relative ability to cleave the following substrates; A: fluorogenic peptide substrate (Mca-PLGL-Dpa-AR-NH2 Fluorogenic Matrix Metalloprotease Substrate, Cat#ES001), B: fluorogenic peptide substrate (Mca-RPKPVE-Nval-WRK(Dnp)-NH2 Fluorogenic MMP Substrate, Cat#ES002) which detects additional metalloprotease activity and Factor X, C: fluorogenic peptide substrate (Mca-PLAQAV-Dpa-RSSSR-NH2 Fluorogenic Peptide Substrate, Cat#ES003) which detects additional metalloprotease activity, D: fluorogenic peptide substrate (Mca-KPLGL-Dpa-AR-NH2 Fluorogenic Peptide Substrate, Cat#ES010) which detects additional metalloprotease activity, E: fluorogenic peptide substrate (Boc-VPR-AMC Fluorogenic Peptide Substrate, Cat#ES011) which detects serine protease activity, F: Phospholipase A_2 substrate activity, EnzChek® (Cat# E10217). Warmer colours represent more potent substrate cleavage. Bars indicate 95% confidence intervals for the estimate at each node. Phylogeny follows (Alencar et al., 2016).

3. Results

3.1. Enzymatic assays on the Fluoroskan Ascent

Enzymatic assays were using substrates typically cleaved by metalloproteases (ES001, ES003, and ES010), serine proteases (ES002 and ES011) or PLA_2. While these are artificial substrates and may not necessarily directly correlate with 'real world' bioactivity, they are useful for elucidating differences between the venoms. Indeed, significant variation was observed between the venoms for each substrate class (Fig. 1). In addition to variation between venoms, there was also significant variation between substrate types, whereby the strongest for one substrate type was not the strongest for another substrate within the same generalized class (whether within the metalloprotease or serine protease class). For ES001 *P. flavoviridis* was twice as active as the next strongest venom (the sister species *P. tokarensis*), and three

times as active as *P. mucrosquamatus* with the other species only showing low levels of activity (Fig. 1A). A broadly similar pattern was observed for ES010, with *P. flavoviridis* being significantly more active than the other venoms, however with some venoms that showed only trace activity upon ES001 showing significant activity upon ES010 (*P. elegans,* and *P. mangshanensis*) (Fig. 1D). In contrast, for ES003 (also a metalloprotease substrate), *P. mucrosquamatus* was much more active than all other venoms, being four times as active as the next potent species (*P. tokarensis*) (Fig. 1C). A similar level of variation between the serine protease substrates was also observed, where *P. elegans* was the most potent, but all other venoms displaying at least moderate levels of activity, while for *P. jerdonii* and *P. mangshanensis* were both potent while all other venoms displayed only trace or undetectable levels of activity (Fig. 1B and E). *P. flavoviridis* displayed the highest activity upon the PLA_2 substrate, with the next nearest venom (*P. elegans*) being 66% as potent, followed by *P. tokarensis* (33%), and all others showing only very low levels of activity (Fig. 1F). These variations are strongly suggestive of differential activity of the venoms under physiological conditions. The extreme variation between species was evident in the ancestral state reconstructions (Fig. 1), which was consistent with rapid diversification away from an ancestral state. The basal lineages *P. jerdonii* and *P. mangshanensis* were inactive on the substrates ES001, ES003, and the PLA_2 substrate, with the respective high levels of activity of *P. flavoviridis* (ES001), *P. mucrosquamatus* (ES003), and *P. flavoviridis* (PLA_2) thus representing derived states (Fig. 1A, C, and F respectively). Conversely the high levels of activity of the two basal lineages *P. jerdonii* and *P. mangshanensis* on ES011 is indicative of this being the ancestral state, with the low levels of the other lineages therefore being derived states (Fig. 1E). In contrast the low level of activity for ES010 by *P. jerdonii* represents a derived state as all other lineages are either moderately potent (*P. elegans, P. mangshanensis, P. mucrosquamatus,* and *P. tokarensis*) or highly potent (*P. flavoviridis*) (Fig. 1D).

3.2. Coagulation analyses

3.2.1. Action upon plasma

3.2.1.1. Plasma clotting and co-factor dependency of Ca^{2+} and phospholipid. Only *P. elegans, P. mangshanensis*, and *P. jerdonii* and displayed the ability to clot human plasma (Fig. 2). At a 20 μg/ml venom concentration, *P. mangshanensis* was able to clot plasma in 32.0 s ± 5.4, compared to *P. elegans* (98.9 s ± 6.66), and *P. jerdonii* (139.0 s ± 11.9) relative to the spontaneous clotting time of the recalcified plasma of 325.0 ± 25.0 s. In contrast, the *P. flavoviridis* and *P. tokarensis* venom demonstrated a potently anticoagulant effect, with both species reaching the machine maximum clotting time measurement of 999.99 s. *P. mucrosquamatus* venom was also anticoagulant at a 20 μg/ml venom concentration but weaker than *P. flavoviridis* and *P. tokarensis* (Fig. 2). The venoms displayed significant variation in the relative dependency upon calcium or phospholipid, with calcium being a much stronger variable (Fig. 2B and C).

As the clotting of plasma could be due to procoagulant functions through the generation of endogenous thrombin (producing strong fibrin clots), or pseudo-procoagulant functions by directly acting upon fibrinogen (producing weak clots), additional tests were conducted to ascertain the ability to activate Factor X or prothrombin, and also to determine the relative strength of fibrin clots in the plasma tests. None of the venoms, even the ones which produced clots in the above analyses, were able to activate FX or PT. Further, the clots formed by the venoms in plasma were weak, indicated by reduced clot strength relative to the controls (Fig. 3). As this was strongly suggestive of direct action upon fibrinogen in a pseudo-procoagulant manner (Oulion et al., 2018), additional tests were undertaken (Results section 2 below) to characterise the cleavage and clotting effects upon fibrinogen.

3.2.1.2. Plasma anticoagulant inhibition – FXa and thrombin. Additional testing was conducted to investigate the anticoagulant properties of the two most potent anticoagulant species, *P. tokarensis* and *P. flavoviridis* based off their initial inability to clot human plasma (Fig. 2). Given that both species failed to form any clot (Fig. 2), their venom components may interfere with specific reactions in the coagulation cascade. FXa inhibition and thrombin inhibition were investigated across a range of concentrations. While both venom species were unable to successfully inhibit thrombin, they were able to inhibit FXa, with *P. flavoviridis* being much more potent than *P. tokarensis* (Fig. 4).

3.2.2. Action upon fibrinogen

As the above tests suggested that the clotting venoms are pseudo-procoagulant in that they are producing weak fibrin clots, additional tests were undertaken to determine the specific effects upon fibrinogen.

3.2.2.1. Fibrin clot formation. Using the same STA-R Max coagulation analyser protocol as above for plasma, we tested the ability of the venoms to form fibrin clots by replacing plasma with 4 mg/ml human fibrinogen. Consistent with the plasma results, and demonstrative of direct effect upon fibrinogen in a pseudo-procoagulant manner, *P. jerdonii* and *P. mangshanensis* venoms were the only ones able to effectively trigger the formation of fibrin clots (Fig. 5). In testing for the relative influence of the physiological cofactors calcium and phospholipid, extensive variation was noted between the cofactors, and also between the species for a particular cofactor. Removal of calcium slowed the reaction, resulting in a 65.1 ± 0.7% increase in the area under the curve for *P. jerdoni*, but the removal of phospholipid had a negligible effect, with the area under the curve increasing by only 6.6 ± 1.8%. In contrast, *P. mangshanensis* showed a 128.9 ± 0.8% increase in the area under the curve when calcium was removed and a 37.2 ± 0.7% increase when phospholipid was removed.

3.2.2.2. Thromboelastography using TEG5000s. In order to determine the strength of the clots formed by fibrinogen cleavage, we investigated the ability for venom to clot fibrinogen in the presence of Ca^{2+} and phospholipid. The thrombin control rapidly (SP = 0.2 +/− 0 min, *R* = 0.23 +/− 0.06 min) produced a strong (13.37 +/− 1.24 mm). While *P. mangshanensis* was the most potent of the venoms, the clot was formed slower (SP = 1.5 +/− 0.4 min, *R* = 2.07 +/− 0.68 min) and weaker (A = 7.33 +/− 1.08) than the thrombin control (SP = 0.2 +/− 0.0 min, R = 0.23 +/− 0.06 min, A = 16.5 +/− 1.2) (Fig. 6). *P. jerdonii* and *P. elegans* also clotted the fibrinogen but slower and weaker than *P. mangshanensis* (Fig. 6).

As *P. flavoviridis, P. mucrosquamatus* and *P. tokarensis* did not display any ability to directly clot fibrinogen, additional tests were undertaken in order to ascertain if the venoms were cleaving the fibrinogen in a destructive manner that impeded the ability of thrombin to clot fibrinogen. Thrombin was added to the wells after the 30 min primary run in which no clot was formed. Consistent with destructive cleavage of fibrinogen by *P. mucrosquamatus* and *P. tokarensis* venoms, the addition of thrombin failed to produce a clot (Fig. 6). In contrast, *P. flavoviridis* displayed a much weaker level of destructive cleavage. As this venom showed a strong anticoagulation activity upon the plasma (Fig. 6), the low activity upon fibrinogen indicates that the anticoagulation activity is due to the direct inhibition of a clotting factor, which is consistent with the results showing an ability to inhibit FXa (Fig. 4).

3.2.2.3. Fibrinogen gels. In order to determine the specific fibrinogen chains cleaved by the venoms, additional assays were undertaken to determine the time-dependent effects upon each chain. A consistent pattern emerged with all venoms displayed the ability to cleave the α chain (with differential potency), while the β chain was cleaved more slowly and only fully cleaved by the most potent α chain acting venoms (Figs. 7-9). Similarly, the γ chain was cleaved more slowly and only cleaved by the most potent α and β chain cleavers. Full cleavage of α, β

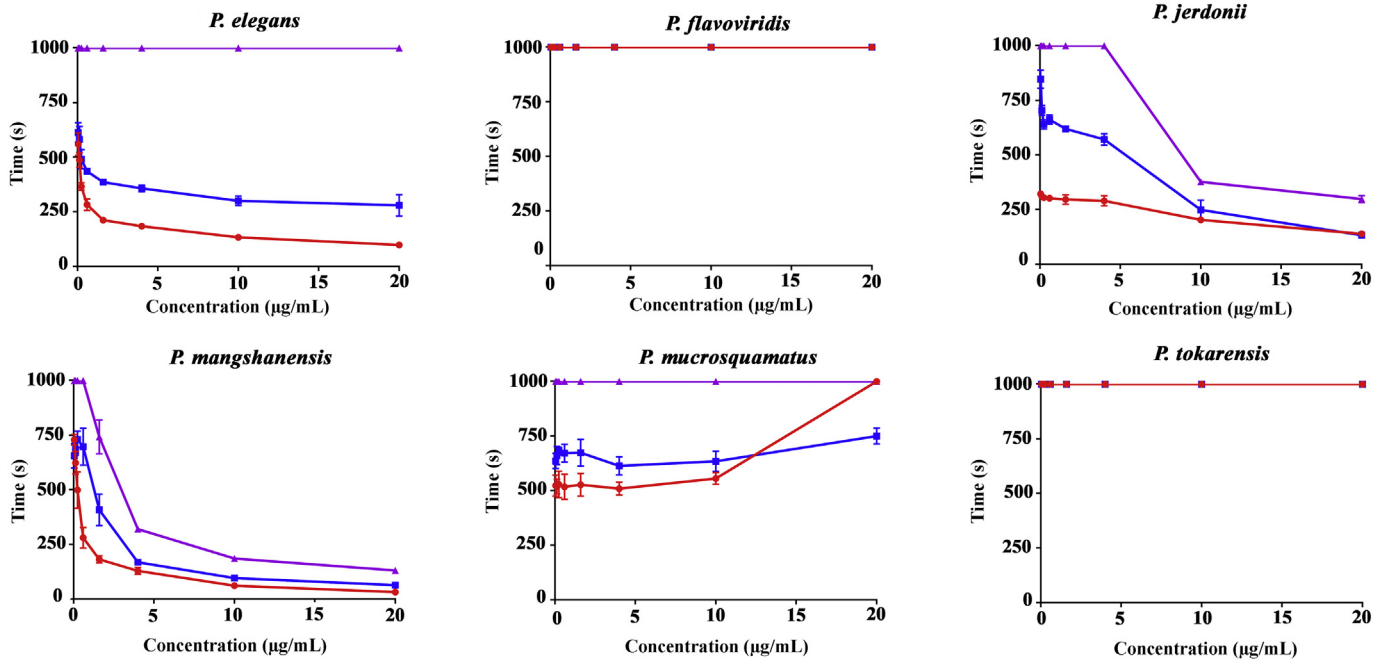

Fig. 2. Comparison of procoagulant co-factor dependency clotting curves of *Protobothrops* at varying venom concentrations on human plasma. *X* axis: final venom concentration (µg/ml), *Y* axis: clotting time in seconds. Data points are *N* = 3 and error bards indicate standard deviation. Red line = procoagulant dilution series with calcium and phospholipid against human plasma. Blue line = Phospholipid dependency, procoagulant dilution series with calcium added only against human plasma. Purple line = Calcium dependency, procoagulant dilution series with phospholipid added only against human plasma. (For interpretation of the references to colour in this figure legend, the reader is referred to the web version of this article.)

and γ fibrinogen chains were only exhibited by *P. jerdonii* and *P. mangshanensis*. *P. mangshanensis* however cleaved all 3 chains much more quickly than *P. jerdonii* (Figs. 6-8). Cleavage of only the α and β chains were exhibited in *P. elegans* and *P. mucrosquamatus*, while *P. flavoviridis* and *P. tokarensis* only exhibited α chain degradation (Figs. 7-9). Ancestral state reconstruction suggested that the ability to cleave the α, β and γ fibrinogen chains was the basal condition, with the other cleavage patterns thus being derivations (Fig. 9), with the pseudo-procoagulant clotting (Fig. 4) being the basal activity of the genus upon fibrinogen.

3.2.2.4. Fibrinolysis +/− tissue plasminogen activator. The ability for *Protobothrops* crude venom to actively lyse a plasma clot was investigated under the presence or absence of tPA (tissue plasminogen activator) at varying concentrations. None of the 6-species tested at any of the concentrations successfully lysed plasma clots without the presence of tPA. However, in the presence of tPA, clot lysis times (CLT) were shortened relative to the control (tPA against plasma) (Fig. 10).

P. mangshanensis, *P. jerdonii*, *P. mucrosquamatus* and *P. elegans* venoms demonstrated a reduced CLT in the presence of tPA as compared

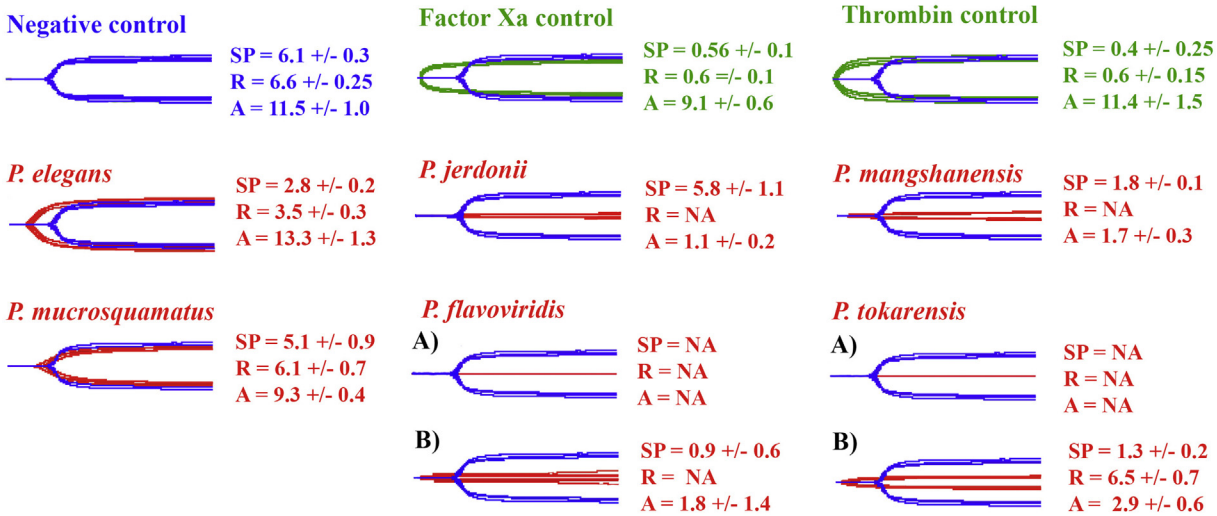

Fig. 3. Overlaid thromboelastography traces showing effects of 20 µg/ml venoms ability to clot plasma relative to spontaneous clot control: blue traces = re-calcified plasma spontaneous clotting control; green traces = Factor Xa or thrombin controls; red traces = venom samples. SP = split point, time taken until clot begins to form. R = time to initial clot formation where formation is 2 mm^{+} (mins). A (parameter) = detectable clot strength (mm) which may be < 2 mm. As *P. flavoviridis* and *P. tokarensis* did not induce a clot in A), thrombin was added in B) in order to induce a clot and measure fibrinogen degradation. Overlaid traces are N = 3 for each set of control or experimental conditions. Values are N = 3 means and standard deviation. NA indicates below machine detection limit. (For interpretation of the references to colour in this figure legend, the reader is referred to the web version of this article.)

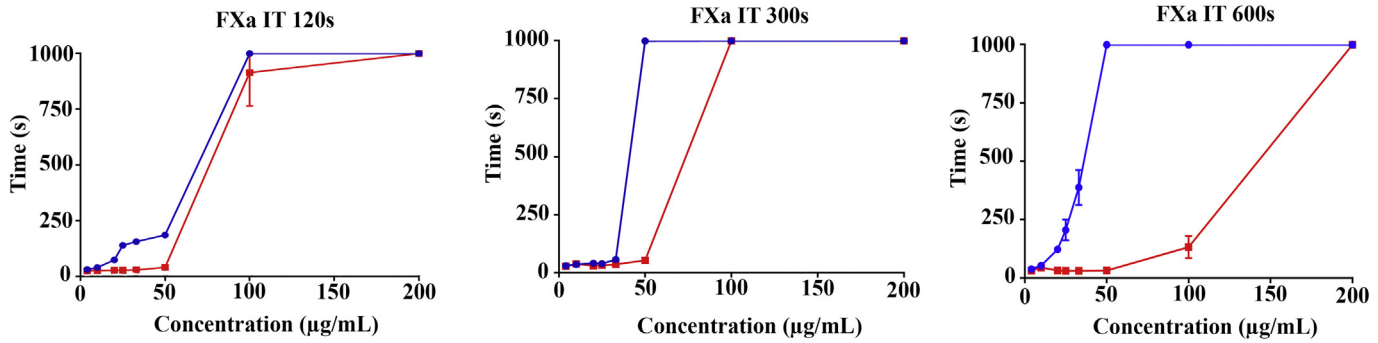

Fig. 4. Factor Xa inhibition tests (FXa IT) for *P. flavoviridis* and *P. tokarensis* measured over 120, 300 and 600 s incubation times. X axis: final venom concentration (µg/ml), Y axis: clotting time in seconds. Data points are N = 3 and error bars indicate standard deviation. Blue line: *P. flavoviridis*. Red line: *P. tokarensis*. (For interpretation of the references to colour in this figure legend, the reader is referred to the web version of this article.)

to the control. Consistent with its potent anticoagulant effect, plasma in the presence of *P. flavoviridis* venom failed to form a clot due to complete degradation by venom at 1 µg concentration.

3.2.3. Platelet agglutination and inhibition

The ability for *Protobothrops* crude venom to agglutinate and inhibit platelets was investigated, with only *P. tokarensis* and *P. flavoviridis* potently inhibiting platelet agglutination (Fig. 11).

4. Discussion

Extensive functional diversification was evident between the six *Protobothrops* venoms tested, both in artificial environments (enzyme substrate testing) and physiological conditions (plasma and fibrinogen testing). This was evident by the ancestral state reconstructions (Figs. 1 and 9) showing rapid diversification away from the basal condition. Enzyme substrate testing patterns were differential between the substrate types tested, whether metalloprotease or serine protease, with no consistent functional or phylogenetic pattern, consistent with rapid radiation away from the ancestral state. While these substrates do not necessarily correlate with a particular physiological effect, the differential activity indicates that the venoms would have highly variable effects in a physiological system. This was shown to be the case with the venoms displaying a wide variation of coagulotoxic activity, ranging from potently pseudo-procoagulant to potently anticoagulant. A correlation, however, was evident between the nature and potency of the coagulotoxicity, with the strongest pseudo-procoagulant venoms (*P. jerdonii* and *P. mangshanensis*) displaying an ability to aberrantly cleave the alpha, beta and gamma chains of fibrinogen, with this putatively being the ancestral state, while the most potent anticoagulant venoms (*P. flavoviridis* and *P. tokarensis*) cleaving only the alpha chain, with this representing an extreme derivation away from the ancestral state, with the anticoagulation potentiated by the derived state of FXa-inhibition. Thromboelastography testing confirmed the pseudo-procoagulant function of *P. jerdonii* and *P. mangshanensis* venoms, with both being the most rapid in clotting fibrinogen but producing only weak clots. As these are the two most basal species (Alencar et al., 2018; Alencar et al., 2016), and the two most potent anticoagulant species are sister to each other, consistent with pseudo-procoagulant activity as the basal condition within this genus, and that anticoagulant venoms represent the derived state.

Consistent with the extreme variation in their venoms, *Protobothrops* species are highly variable in morphology and ecological niche occupied, ranging from heavily built terrestrial species (eg *P. mangshanensis*) to gracile semi-arboreal species (eg *P. flavoviridis*). While the venom variation is suggestive of this feature being a driver in their adaptive radiation, it is also indicative of the potential to produce differential clinical effects, in that while haemorrhagic shock may be produced by all (Chen et al., 2009; Nishimura et al., 2016), the underlying mechanics may be different.

In addition to net anticoagulation produced by direct action upon fibrinogen (whether pseudo-procoagulant or anticoagulant), anticoagulation was also produced by these venoms as a by-product of irregular fibrinogen cleavage. This was evident in the fibrinolysis assays, whereby plasmin was able to lyse clots much quicker when venom from species was present (Fig. 10). It is hypothesised that this is due to venoms from some species forming a weak clot via incorrect fibrinogen degradation and irregular fibrin strand linking. This has been

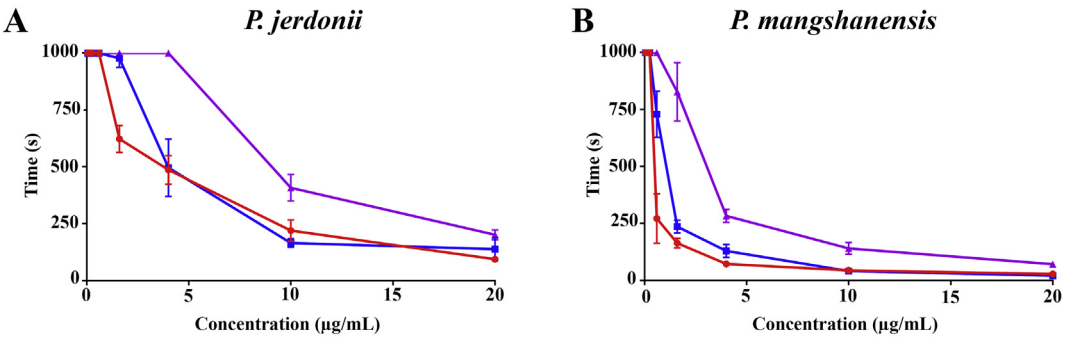

Fig. 5. Comparison of procoagulant co-factor dependency clotting curves of two *Protobothrops* species at varying venom concentrations on human fibrinogen (4 mg/ml). *X* axis: final venom concentration (µg/ml), *Y* axis: clotting time in seconds. A = *P. jerdonii*, B = *P. mangshanensis*. Red line: procoagulant dilution series with calcium and phospholipid against human fibrinogen, Blue line: procoagulant dilution series with calcium only against human fibrinogen, Purple line: procoagulant dilution series with phospholipid only against human fibrinogen. Data points are N=3 and error bars indicate standard deviation. Area under the curve: for A = calcium dependency 0.651 ± 0.068, phospholipid dependency 0.066 ± 0.018. For B = calcium dependency 1.289 ± 0.008, phospholipid dependency 0.372 ± 0.007. (For interpretation of the references to colour in this figure legend, the reader is referred to the web version of this article.)

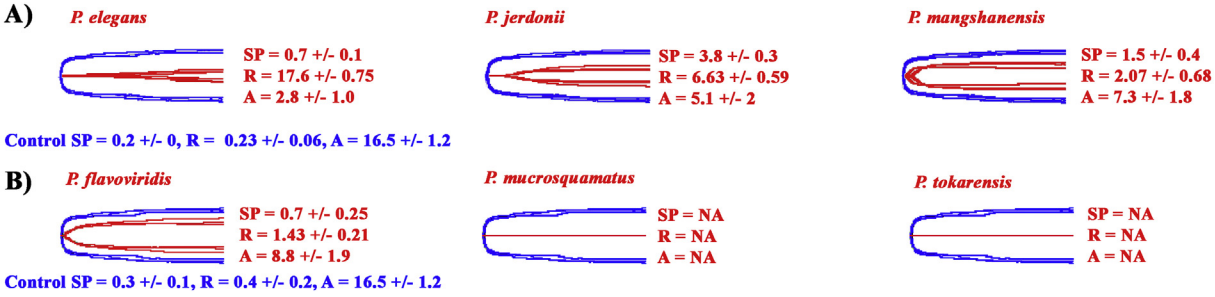

Fig. 6. Overlaid thromboelastography traces showing effects of 20 μg/ml venoms: A) ability to clot fibrinogen relative to thrombin control; B) ability to clot whereby thrombin was added to samples which did not clot fibrinogen after 30 min in order to test for venom-induced fibrinogen degradation relative to blank control. Blue traces = thrombin controls, red traces = venom samples. SP = split point, time taken until clot begins to form. R = time to initial clot formation where formation is 2 mm + (mins). A (parameter) = detectable clot strength (mm) which may be < 2 mm. Overlaid traces are N = 3 for each set of control or experimental conditions. Values are N = 3 means and standard deviation. (For interpretation of the references to colour in this figure legend, the reader is referred to the web version of this article.)

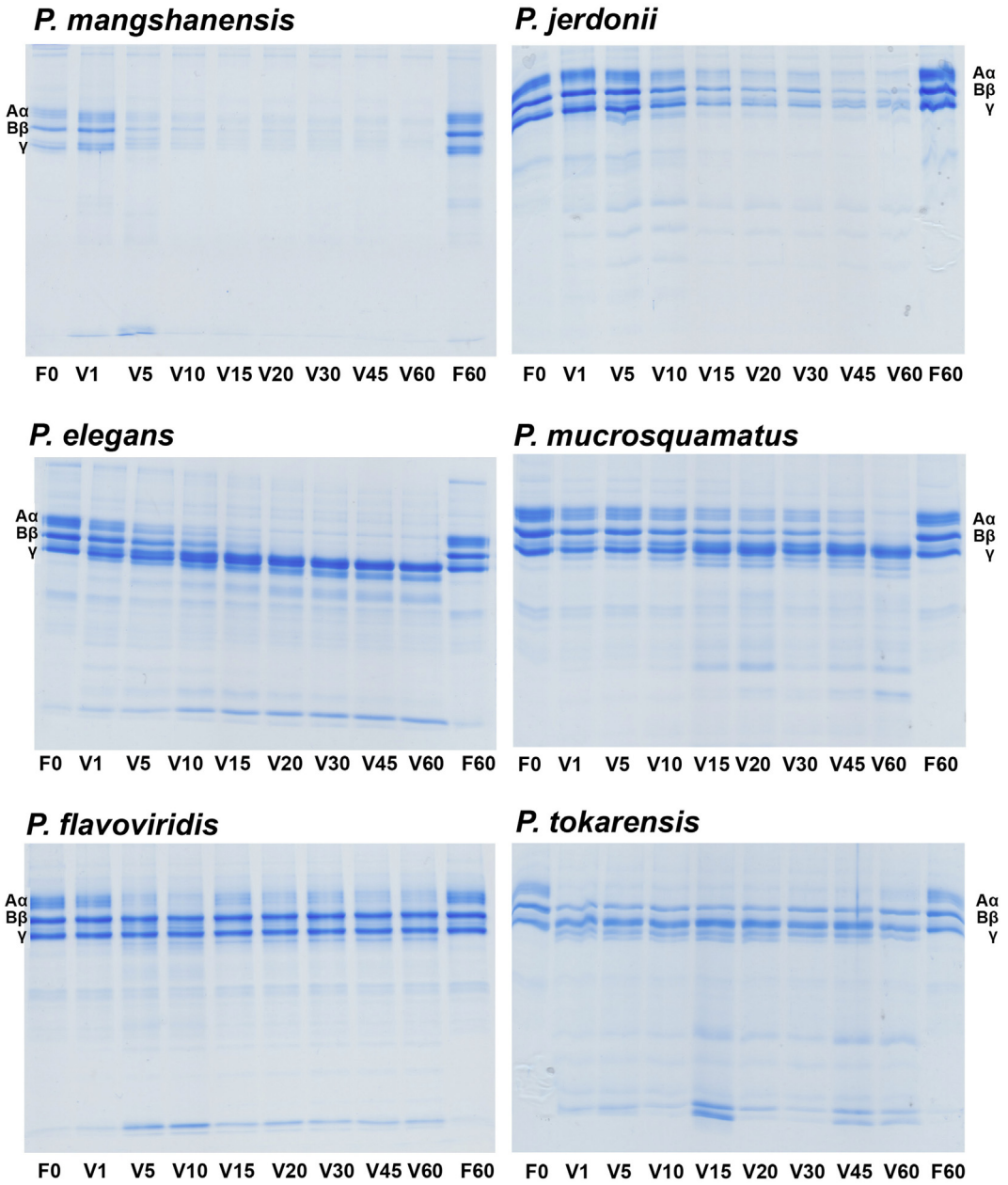

Fig. 7. 1D SDS PAGE time dependent fibrinogen chain degradation (α, β or γ) by venom at 0.1 μg/μl concentration, with the fibrinogen at 1 μg/μl, at 37 °C over 60 mins. F = fibrinogen at 0 mins or 60 mins incubation controls, V = venom incubation times (min).

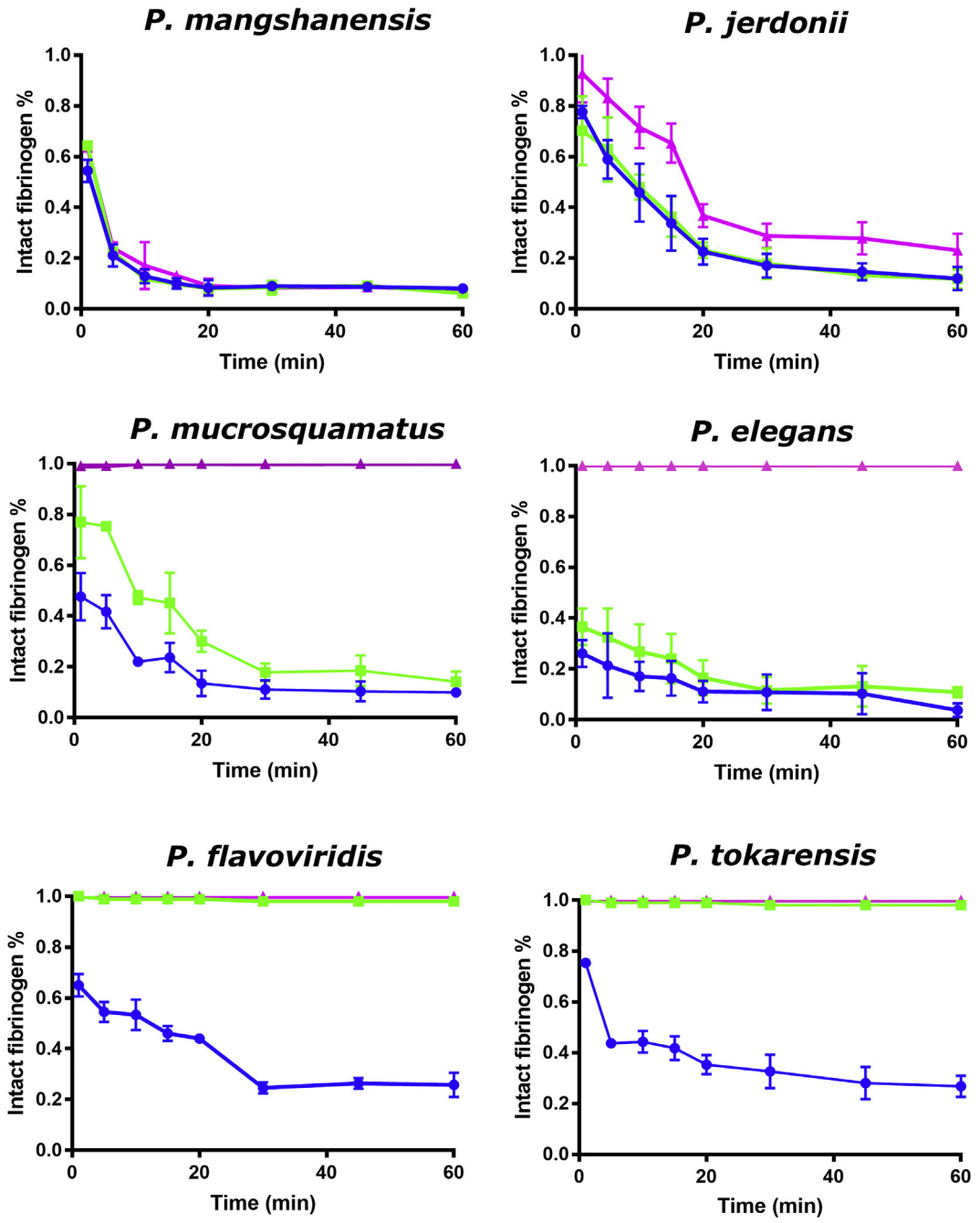

Fig. 8. Relative cleavage of alpha (blue), beta (green) or gamma (pink) chains of fibrinogen. X-axis is time (min), y-axis is percentage of intact chain remaining. Data points are N = means and error bars indicate standard deviation. (For interpretation of the references to colour in this figure legend, the reader is referred to the web version of this article.)

demonstrated in the literature that fibrin diameter and the architecture of the fibrin strands can influence the clot strength and stability (Collet et al., 2000; Longstaff and Kolev, 2015; Mosesson, 2005; Wolberg, 2007; Wolberg and Campbell, 2008). Albeit both species are able to cleave all three fibrinogen chains, fibrinogen is cleaved in incorrect places, as opposed to where thrombin cleaves fibrinogen. This would result in larger fibrin strands which do not form a well-constructed clot and instead form a turbid, highly permeable clot (Collet et al., 2000; Wolberg, 2007; Wolberg and Campbell, 2008). In addition, FXIII is not activated and covalent cross linking, which would also strengthen clots, does not occur. This overall activity would result in a net anticoagulant outcome, despite neither species being able to activate plasminogen, which would aid in this weak anticoagulant effect.

In addition to their wide-ranging fibrinogen action, co-factor dependency of fibrinogen action also impacts on the physiological degree of fibrinogenolysis that the venom exhibits. The co-factor dependency of the two most potent species, *P. jerdonii* and *P. mangshanensis*, shows that not only does the effect on fibrinogen differ, but also the degree of co-factor dependency for either calcium or phospholipid and between the two species for a particular co-factor. This is the first study to show such an extensive shift in co-factor dependency on fibrinogen action from any snake species, illustrating that not only does the co-factor dependency differ but it also differs between species of a single genus. This reinforces the fundamental importance of including both co-factors in order to replicate physiological conditions. While some venom studies have done this (Bos et al., 2016; Chester and Crawford, 1982;

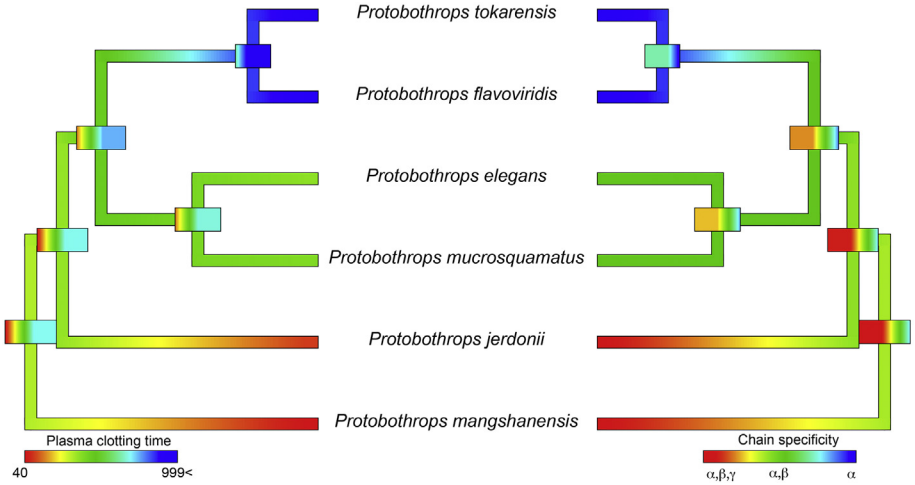

Fig. 9. Ancestral state reconstruction of coagulation clotting times on human plasma relative to fibrinogen chain cleavage specificity. Bars indicate 95% confidence intervals for the estimate at each node. Phylogeny follows (Alencar et al., 2016).

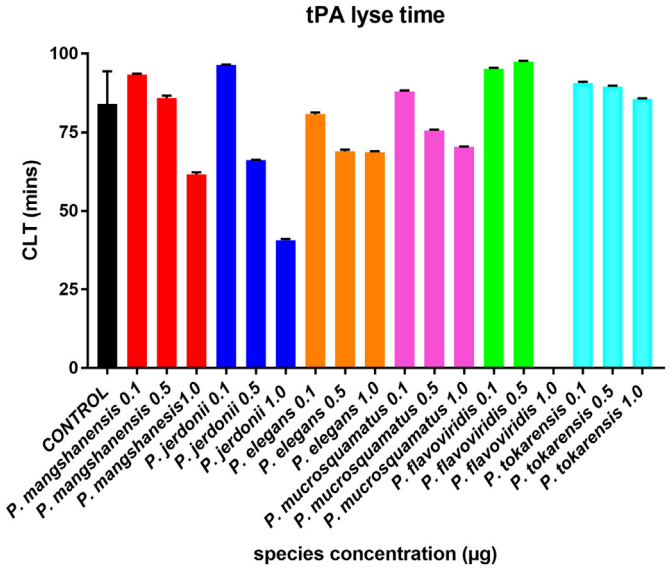

Fig. 10. Clot lysis Time (CLT) for each *Protobothrops* species in the presence of tPA at 0.1 µg, 0.5 µg and 1 µg venom concentrations. Control is indicated in black. Data points are N = 3 and error bars indicate standard deviation. Bars which are lower than the control lysed the plasma clot quicker than under normal tPA conditions.

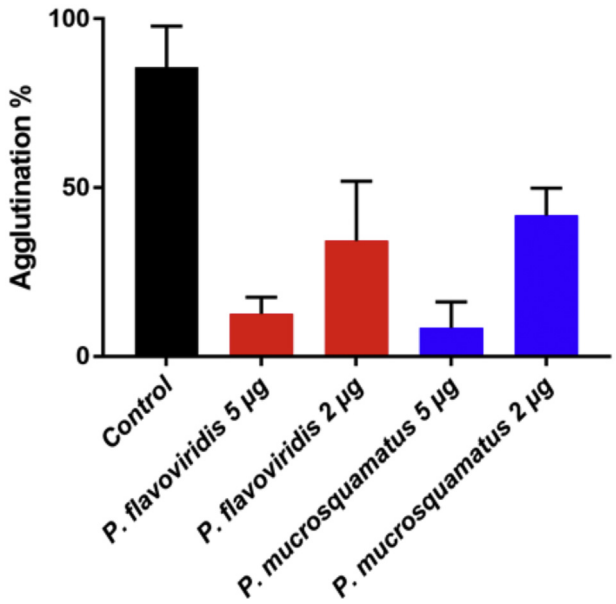

Fig. 11. Platelet agglutination inhibition at 5 µg and partial inhibition at 2 µg for *P. flavoviridis* and *P. tokarensis*. Black column indicates control run, red column indicates *Protobothrops* flavoviridis, blue column indicates *Protobothrops* mucrosquamatus run. Y axis: platelet agglutination percentage. Data points are N = 3 and error bars indicate standard deviation. (For interpretation of the references to colour in this figure legend, the reader is referred to the web version of this article.)

Debono et al., 2017; Lister et al., 2017; Oulion et al., 2018; Pirkle et al., 1972; Rogalski et al., 2017), the inclusion of which is necessary to replicate physiological conditions, while others have neglected to include phospholipid (Isbister et al., 2010; Nielsen et al., 2018; O'Leary and Isbister, 2010; Still et al., 2017; Vargas et al., 2011), or both cofactors (Ainsworth et al., 2018; Resiere et al., 2018; Williams et al., 1994) thereby skewing the results and hampering the interpretation as to the effects upon coagulation and therefore limiting the clinical and evolutionary relevance of the results.

In addition to this variation in net anticoagulation produced, it was shown that the two most potent anticoagulant species of the genus, *P. flavoviridis* and *P. tokarensis* (those that did not form a plasma or fibrinogen clot) also inhibited FXa (Fig. 4). FX inhibition has been described previously by *P. flavoviridis* due to lectin toxins (Arlinghaus et al., 2015; Atoda et al., 1995) while it had not been previously described for *P. tokarensis*. As none of the more basal venoms displayed this activity, but it is known from other pitviper venoms (Arlinghaus et al., 2015), this suggests that the ability to inhibit FXa was present in only trace levels in the last common ancestor of all *Protobothrops* species but was upregulated in the last common ancestor of *P. flavoviridis* and *P. tokarensis*.

This continued variation in venom activity, enzymatic activity, functional diversification and clotting diversification creates further problems with predictive antivenom production raised against specific species, or species of a specific region. At present there are only two antivenoms that are produced for two of the eight species of *Protobothrops*, registered for *P. mucrosquamatus* and *P. flavoviridis*, with no available antivenom specifically made for the remainder of the genus. The two *Protobothrops* antivenoms are the 'Bivalent Antivenin Pit Viper, National Institute of Preventative Medicine, Taiwan', produced from *P. mucrosquamatus* and *Trimeresurus stejnegeri*, and the 'Habu Antivenom (Kaketsuken), by the Chemo-Sero-Therapeutic Research Institute (Kaketsuken), Japan', produced from *P. flavoviridis*. Future

works should investigate the ability of these antivenoms to specifically neutralise coagulotoxic effects and to what degree the antivenoms cross-react with non-immunising venoms. This is particularly critical for *P. jerdonii* and *P. mangshanensis* which differ sharply in their coagulotoxic biochemistry relative to either of the *Protobothrops* venoms used in antivenom production (*P. flavoviridis* and *P. mucrosquamatus*). This study therefore not only reveals evolutionary trends of interest to biologists, but also documents substantial variation in the nature and potency of coagulotoxic effects that would directly inform upon potential clinical effects and management strategies.

Acknowledgements

HFK was supported by the Science and Technology Development Fund of Macau SAR (FDCT) [019/2017/A1].

References

Ainsworth, S., Slagboom, J., Alomran, N., Pla, D., Alhamdi, Y., King, S.I., Bolton, F.M., Gutiérrez, J.M., Vonk, F.J., Toh, C.-H., 2018. The paraspecific neutralisation of snake venom induced coagulopathy by antivenoms. Communicat. Biol. 1, 34.

Alencar, L.R., Quental, T.B., Grazziotin, F.G., Alfaro, M.L., Martins, M., Venzon, M., Zaher, H., 2016. Diversification in vipers: Phylogenetic relationships, time of divergence and shifts in speciation rates. Mol. Phylogenet. Evol. 105, 50–62.

Alencar, L.R., Martins, M., Greene, H.W., 2018. Evolutionary History of Vipers. eLS. pp. 1–10.

Ali, S.A., Yang, D.C., Jackson, T.N., Undheim, E.A., Koludarov, I., Wood, K., Jones, A., Hodgson, W.C., McCarthy, S., Ruder, T., Fry, B.G., 2013. Venom proteomic characterization and relative antivenom neutralization of two medically important Pakistani elapid snakes (*Bungarus sindanus* and *Naja naja*). J. Proteome 89, 15–23.

Arlinghaus, F.T., Fry, B.G., Sunagar, K., Jackson, T.N.W., Eble, J.A., Reeks, T., Clemetson, K.J., 2015. Lectin Proteins, Venomous Reptiles and their Toxins. Oxford University Press, New York.

Atoda, H., Ishikawa, M., Yoshihara, E., Sekiya, F., Morita, T., 1995. Blood coagulation factor IX-binding protein from the venom of *Trimeresurus flavoviridis*: purification and characterization. J. Biochem. 118, 965–973.

Bagoly, Z., Koncz, Z., Hársfalvi, J., Muszbek, L., 2012. Factor XIII, clot structure, thrombosis. Thromb. Res. 129, 382–387.

Bos, M.H., Van't Veer, C., Reitsma, P.H., 2016. Molecular biology and biochemistry of the coagulation factors and pathways of hemostasis. In: Kaushansky, K., Lichtman, M.A., Prchal, J.T., Levi, M.M., Press, O.W., Burns, L.J., Caligiuri, M. (Eds.), Williams Hematology, 9th ed. .

Cascardi, J., Young, B.A., Husic, H.D., Sherma, J., 1999. Protein variation in the venom spat by the red spitting cobra, *Naja pallida* (Reptilia: Serpentes). Toxicon 37, 1271–1279.

Casewell, N.R., Wüster, W., Vonk, F.J., Harrison, R.A., Fry, B.G., 2013. Complex cocktails: the evolutionary novelty of venoms. Trends Ecol. Evol. 28, 219–229.

Casewell, N.R., Sunagar, K., Takacs, Z., Calvete, J.J., Jackson, T.N.W., Fry, B.G., 2015. Snake Venom Metalloprotease Enzymes, Venomous Reptiles and their Toxins. Oxford University Press, New York.

Chen, Y.W., Chen, M.H., Chen, Y.C., Hung, D.Z., Chen, C.K., Yen, D.H.T., Huang, C.I., Lee, C.H., Wang, L.M., Yang, C.C., 2009. Differences in clinical profiles of patients with *Protobothrops mucrosquamatus* and *Viridovipera stejnegeri* envenoming in Taiwan. The Am. J. Trop. Med, Hygiene 80, 28–32.

Chester, A., Crawford, G., 1982. In vitro coagulant properties of venoms from Australian snakes. Toxicon 20, 501–504.

Collet, J., Park, D., Lesty, C., Soria, J., Soria, C., Montalescot, G., Weisel, J., 2000. Influence of fibrin network conformation and fibrin fiber diameter on fibrinolysis speed. Arterioscler. Thromb. Vasc. Biol. 20, 1354–1361.

Daltry, J.C., Wuster, W., Thorpe, R.S., 1996. Diet and snake venom evolution. Nature 379, 537.

Debono, J., Dobson, J., Casewell, N.R., Romilio, A., Li, B., Kurniawan, N., Mardon, K., Weisbecker, V., Nouwens, A., Kwok, H.F., 2017. Coagulating Colubrids: Evolutionary, Pathophysiological and Biodiscovery Implications of Venom Variations between Boomslang (*Dispholidus typus*) and Twig Snake (*Thelotornis mossambicanus*). Toxins 9, 171.

Deufel, A., Cundall, D., 2003. Feeding in *Atractaspis* (Serpentes: Atractaspididae): a study in conflicting functional constraints. Zoology 106, 43–61.

Fry, B.G., 2005. From genome to "venome": molecular origin and evolution of the snake venom proteome inferred from phylogenetic analysis of toxin sequences and related body proteins. Genome Res. 15, 403–420.

Fry, B.G., Wüster, W., 2004. Assembling an arsenal: origin and evolution of the snake venom proteome inferred from phylogenetic analysis of toxin sequences. Mol. Biol. Evol. 21, 870–883.

Fry, B.G., Scheib, H., van der Weerd, L., Young, B., McNaughtan, J., Ramjan, S.R., Vidal, N., Poelmann, R.E., Norman, J.A., 2008. Evolution of an arsenal structural and functional diversification of the venom system in the advanced snakes (Caenophidia). Mol. Cell. Proteomics 7, 215–246.

Fry, B.G., Roelants, K., Champagne, D.E., Scheib, H., Tyndall, J.D., King, G.F., Nevalainen, T.J., Norman, J.A., Lewis, R.J., Norton, R.S., Renjifo, C., Rodríguez De La Vega, R.C., 2009a. The toxicogenomic multiverse: convergent recruitment of proteins into animal venoms. Annu. Rev. Genomics Hum. Genet. 10, 483–511.

Fry, B.G., Vidal, N., Van der Weerd, L., Kochva, E., Renjifo, C., 2009b. Evolution and diversification of the Toxicofera reptile venom system. J. Proteome 72, 127–136.

Fry, B.G., Undheim, E.A., Ali, S.A., Jackson, T.N., Debono, J., Scheib, H., Ruder, T., Morgenstern, D., Cadwallader, L., Whitehead, D., Nabuurs, R., van der Weerd, L., Vidal, N., Roelants, K., Hendrikx, I., Pineda Gonzalez, S., Koludarov, I., Jones, A., King, G.F., Antunes, A., Sunagar, K., 2013. Squeezers and leaf-cutters: differential diversification and degeneration of the venom system in toxicoferan reptiles. Mol. Cell. Proteomics 12, 1881–1899.

Hayes, W.K., Herbert, S.S., Harrison, J.R., Wiley, K.L., 2008. Spitting versus biting: differential venom gland contraction regulates venom expenditure in the black-necked spitting cobra, *Naja nigricollis nigricollis*. J. Herpetol. 42, 453–460.

Isbister, G.K., Woods, D., Alley, S., O'Leary, M.A., Seldon, M., Lincz, L.F., 2010. Endogenous thrombin potential as a novel method for the characterization of procoagulant snake venoms and the efficacy of antivenom. Toxicon 56, 75–85.

Jackson, T.N., Fry, B.G., 2016. A tricky trait: applying the fruits of the "function debate" in the philosophy of biology to the "venom debate" in the science of toxinology. Toxins 8, 263.

Jackson, T.N., Sunagar, K., Undheim, E.A., Koludarov, I., Chan, A.H., Sanders, K., Ali, S.A., Hendrikx, I., Dunstan, N., Fry, B.G., 2013. Venom down under: dynamic evolution of Australian elapid snake toxins. Toxins 5, 2621–2655.

Jackson, T.N., Young, B., Underwood, G., McCarthy, C.J., Kochva, E., Vidal, N., van der Weerd, L., Nabuurs, R., Dobson, J., Whitehead, D., Vonk, F.J., Hendrikx, I., Hay, C., Fry, B.G., 2017. Endless forms most beautiful: the evolution of ophidian oral glands, including the venom system, and the use of appropriate terminology for homologous structures. Zoomorphology 136, 107–130.

Kini, R.M., 2005. Serine proteases affecting blood coagulation and fibrinolysis from snake venoms. Pathophysiol. Haemost. Thromb. 34, 200–204.

Kini, R.M., Koh, C.Y., 2016. Metalloproteases Affecting Blood Coagulation, Fibrinolysis and Platelet Aggregation from Snake Venoms: Definition and Nomenclature of Interaction Sites. Toxins 8, 284.

Koh, C.Y., Kini, R.M., 2012. From snake venom toxins to therapeutics–cardiovascular examples. Toxicon 59, 497–506.

Kolev, K., Longstaff, C., 2016. Bleeding related to disturbed fibrinolysis. Br. J. Haematol. 175, 12–23.

Koludarov, I., Jackson, T.N., Sunagar, K., Nouwens, A., Hendrikx, I., Fry, B.G., 2014. Fossilized venom: the unusually conserved venom profiles of Heloderma species (beaded lizards and gila monsters). Toxins 6, 3582–3595.

Koludarov, I., Jackson, T.N., Dobson, J., Dashevsky, D., Arbuckle, K., Clemente, C.J., Stockdale, E.J., Cochran, C., Debono, J., Stephens, C., Panagides, N., Li, B., Manchadi, M.-L.R., Violette, A., Fourmy, R., Hendrikx, I., Nouwens, A., Clements, J., Martelli, P., Kwok, H.F., Fry, B.G., 2017. Enter the dragon: the dynamic and multifunctional evolution of anguimorpha lizard venoms. Toxins 9, 242.

Li, M., Fry, B., Kini, R.M., 2005. Eggs-only diet: its implications for the toxin profile changes and ecology of the marbled sea snake (*Aipysurus eydouxii*). J. Mol. Evol. 60, 81–89.

Lister, C., Arbuckle, K., Jackson, T.N., Debono, J., Zdenek, C.N., Dashevsky, D., Dunstan, N., Allen, L., Hay, C., Bush, B., Gillett, A., Fry, B.G., 2017. Catch a tiger snake by its tail: Differential toxicity, co-factor dependence and antivenom efficacy in a procoagulant clade of Australian venomous snakes. Comparative Biochem. Phys. Part C 202, 39–54.

Longstaff, C., Kolev, K., 2015. Basic mechanisms and regulation of fibrinolysis. J. Thromb. Haemost. 13.

Mosesson, M., 2005. Fibrinogen and fibrin structure and functions. J. Thromb. Haemost. 3, 1894–1904.

Nelsen, D.R., Nisani, Z., Cooper, A.M., Fox, G.A., Gren, E.C., Corbit, A.G., Hayes, W.K., 2014. Poisons, toxungens, and venoms: redefining and classifying toxic biological secretions and the organisms that employ them. Biol. Rev. 89, 450–465.

Nielsen, V.G., Frank, N., Matika, R.W., 2018. Carbon monoxide inhibits hemotoxic activity of Elapidae venoms: potential role of heme. Biometals 31, 51–59.

Nishimura, H., Enokida, H., Kawahira, S., Kagara, I., Hayami, H., Nakagawa, M., 2016. Acute kidney injury and rhabdomyolysis after *Protobothrops flavoviridis* bite: a retrospective survey of 86 patients in a tertiary care center. The Am. J. Trop. Med, Hygiene 94, 474–479.

O'Leary, M.A., Isbister, G.K., 2010. A turbidimetric assay for the measurement of clotting times of procoagulant venoms in plasma. J. Pharmacol. Toxicol. Methods 61, 27–31.

Oulion, B., Dobson, J.S., Zdenek, C.N., Arbuckle, K., Lister, C., Coimbra, F.C., Op den Brouw, B., Debono, J., Rogalski, A., Violette, A., Fourmy, R., Frank, N., Fry, B.G., 2018. Factor X activating *Atractaspis* snake venoms and the relative coagulotoxicity neutralising efficacy of African antivenoms. Toxicol. Lett. 288, 119–128.

Panagides, N., Jackson, T.N., Ikonomopoulou, M.P., Arbuckle, K., Pretzler, R., Yang, D.C., Ali, S.A., Koludarov, I., Dobson, J., Sanker, B., Asselin, A., Santana, R.C., Hendrikx, I., van der Ploeg, H., Tai-A-Pin, J., van den Bergh, R., Kerkkamp, H.M.I., Vonk, F.J., Naude, A., Strydom, M.A., Jacobsz, L., Dunstan, N., Jaeger, M., Hodgson, W.C., Miles, J., Fry, B.G., 2017. How the cobra got its flesh-eating venom: Cytotoxicity as a defensive innovation and its co-evolution with hooding, aposematic marking, and spitting. Toxins 9, 103.

Paradis, E., Claude, J., Strimmer, K., 2004. APE: analyses of phylogenetics and evolution in R language. Bioinformatics 20, 289–290.

Pawlak, J., Mackessy, S.P., Fry, B.G., Bhatia, M., Mourier, G., Fruchart-Gaillard, C., Servent, D., Ménez, R., Stura, E., Ménez, A., 2006. Denmotoxin, a three-finger toxin from the colubrid snake *Boiga dendrophila* (Mangrove Catsnake) with bird-specific activity. J. Biol. Chem. 281, 29030–29041.

Pawlak, J., Mackessy, S.P., Sixberry, N.M., Stura, E.A., Le Du, M.H., Ménez, R., Foo, C.S., Ménez, A., Nirthanan, S., Kini, R.M., 2009. Irditoxin, a novel covalently linked

heterodimeric three-finger toxin with high taxon-specific neurotoxicity. FASEB J. 23, 534–545.
Pirkle, H., McIntosh, M., Theodor, I., Vernon, S., 1972. Activation of prothrombin with Taipan snake venom. Thromb. Res. 1, 559–567.
Resiere, D., Arias, A.S., Villalta, M., Rucavado, A., Brouste, Y., Cabié, A., Névière, R., Césaire, R., Kallel, H., Mégarbane, B., Mehdaoui, H., Gutiérrez, J.M., 2018. Preclinical evaluation of the neutralizing ability of a monospecific antivenom for the treatment of envenomings by *Bothrops lanceolatus* in Martinique. Toxicon 148, 50–55.
Revell, L.J., 2012. Phytools: an R package for phylogenetic comparative biology (and other things). Methods Ecol. Evol. 3, 217–223.
Rogalski, A., Soerensen, C., Op den Brouw, B., Lister, C., Dashevsky, D., Arbuckle, K., Gloria, A., Zdenek, C.N., Casewell, N.R., Gutiérrez, J.M., Wüster, W., Ali, S.A., Masci, P., Rowley, P., Frank, N., Fry, B.G., 2017. Differential procoagulant effects of saw-scaled viper (Serpentes: Viperidae: *Echis*) snake venoms on human plasma and the narrow taxonomic ranges of antivenom efficacies. Toxicol. Lett. 280, 159–170.
Ryan, E.A., Mockros, L.F., Weisel, J.W., Lorand, L., 1999. Structural origins of fibrin clot rheology. Biophys. J. 77, 2813–2826.
Sajevic, T., Leonardi, A., Križaj, I., 2011. Haemostatically active proteins in snake venoms. Toxicon 57, 627–645.
Schneider, C.A., Rasband, W.S., Eliceiri, K.W., 2012. NIH image to ImageJ: 25 years of image analysis. Nat. Methods 9, 671.
Still, K., Nandlal, R.S., Slagboom, J., Somsen, G.W., Casewell, N.R., Kool, J., 2017. Multipurpose HTS coagulation analysis: assay development and assessment of coagulopathic snake venoms. Toxins 9, 382.
Sunagar, K., Jackson, T.N., Undheim, E.A., Ali, S.A., Antunes, A., Fry, B.G., 2013. Three-fingered RAVERs: Rapid accumulation of variations in exposed residues of snake venom toxins. Toxins 5, 2172–2208.
Sunagar, K., Undheim, E.A., Scheib, H., Gren, E.C., Cochran, C., Person, C.E., Koludarov, I., Kelln, W., Hayes, W.K., King, G.F., Antunes, A., Fry, B.G., 2014. Intraspecific venom variation in the medically significant Southern Pacific Rattlesnake (*Crotalus oreganus helleri*): biodiscovery, clinical and evolutionary implications. J. Proteome 99, 68–83.
Swenson, S., Markland, F., 2005. Snake venom fibrin (ogen) olytic enzymes. Toxicon 45, 1021–1039.
Team, R.C., 2016. R: A Language and Environment for Statistical Computing, 3.3.1 Ed. R Foundation for Statistical Computing, Vienna, Austria.
Vaiyapuri, S., Sunagar, K., Gibbins, J.M., Jackson, T.N.W., Reeks, T., Fry, B.G., 2015. Kallikrein Enzymes, Venomous Reptiles and their Toxins. Oxford University Press, New York.
Vargas, M., Segura, A., Herrera, M., Villalta, M., Estrada, R., Cerdas, M., Paiva, O., Matainaho, T., Jensen, S.D., Winkel, K.D., 2011. Preclinical evaluation of caprylic acid-fractionated IgG antivenom for the treatment of Taipan (*Oxyuranus scutellatus*) envenoming in Papua New Guinea. PLoS Negl. Trop. Dis. 5, e1144.
Vonk, F.J., Casewell, N.R., Henkel, C.V., Heimberg, A.M., Jansen, H.J., McCleary, R.J., Kerkkamp, H.M., Vos, R.A., Guerreiro, I., Calvete, J.J., 2013. The king cobra genome reveals dynamic gene evolution and adaptation in the snake venom system. Proc. Natl. Acad. Sci. 110, 20651–20656.
Williams, V., White, J., Mirtschin, P., 1994. Comparative study on the procoagulant from the venom of Australian brown snakes (Elapidae; *Pseudonaja* spp.). Toxicon 32, 453–459.
Wolberg, A.S., 2007. Thrombin generation and fibrin clot structure. Blood Rev. 21, 131–142.
Wolberg, A.S., Campbell, R.A., 2008. Thrombin generation, fibrin clot formation and hemostasis. Transfus. Apher. Sci. 38, 15–23.
Yang, D.C., Deuis, J.R., Dashevsky, D., Dobson, J., Jackson, T.N., Brust, A., Xie, B., Koludarov, I., Debono, J., Hendrikx, I., Hodgson, W.C., Josh, P., Nouwens, A., Baillie, G.J., Bruxner, T.J.C., Alewood, P.F., Kok Peng Lim, K., Frank, N., Vetter, I., Fry, B.G., 2016. The snake with the scorpion's sting: Novel three-finger toxin sodium channel activators from the venom of the long-glanded blue coral snake (*Calliophis bivirgatus*). Toxins 8, 303.